

# Compact Surface-Normal Coupled Optical Interconnects with Wavelength-Division-Demultiplexing Capability

Suning Tang, Ray T. Chen, M. M. Li, S. Natarajan, R. Mayer, and L. A. Graham  
 Microelectronics Research Center  
 University of Texas at Austin,  
 Austin, Texas 78712-1084  
 Tel: 512-4717035

**Abstract--** We present a novel surface-normal optical wavelength-division-demultiplexer (WDDM), working at 750, 770, 790, 810, 830 and 850 nm wavelengths. The device is based on an integration of a planar waveguide, a substrate waveguide and waveguide holograms. The unique optical in-plane to surface-normal conversion converts the difficult three spatial and three angular edge coupling problem into a planar surface one, resulting in a practical compact face-to-face packaging between the photodetector array and the demultiplexer. A six-channel wavelength-division-demultiplexer with equally spaced collinear surface-normal outputs are designed and demonstrated in a polymer-based planar waveguide in conjunction with holograms on a glass substrate.

It is an established strategy to employ wavelength division multiplexing (WDM) techniques for increasing network capability and functionality. As one of the key optoelectronic components, many types of optical wavelength division demultiplexer (WDDM) have been proposed and demonstrated. These include integrated Mach-Zehnder demultiplexers<sup>[1,2]</sup>, waveguide grating demultiplexer<sup>[3,4]</sup>, and holographic grating demultiplexer<sup>[5-7]</sup>. Since all these demultiplexers are fabricated or packed in a planarized geometry, while the photodetector array employed receive optical signals perpendicular to the substrate surface in most cases, the optoelectronic packaging associated with the array of photodetectors is very challenging and expensive. Precise angular and spatial control is required for both optical coupling and packaging. A wavelength division demultiplexer with the optical in-plane to surface-normal conversion can be a very useful approach to provide effective optical coupling and stacked packaging between an in-plane WDDM and a photodetector array.

In this paper, we present a novel optical wavelength-division-demultiplexer with the unique optical in-plane to surface-normal conversion capability. The device is based on integrating a planar waveguide, a substrate waveguide and waveguide holograms, which provides a compact miniaturized face-to-face packaging between the photodetector array and planar optical channel devices. The optical wavelength-division-demultiplexing is provided by multiplexed holograms in planar waveguide region, and the optical in-plane to surface-normal conversion is conducted within the substrate through substrate surface holograms. The conversion of a planar guided mode to substrate modes generates an additional degree of freedom in designing integrated optical wavelength-division-demultiplexer. More importantly, precise angular control is no longer required for the optical coupling and packaging associated with the photodetector array. To our best knowledge, it is the first

compact optical wavelength-division-demultiplexer that provides the optical in-plane to surface-normal conversion.

The schematic diagram of the device is shown in Fig. 1. It consists of a polymer-based planar waveguide fabricated on the surface of a light transparent substrate. Multiplexed waveguide holograms are employed at the end of the planar waveguide, to convert the planar guided wave into substrate guided modes preserving total internal reflection (TIR). The bouncing angle designed is different for each wavelength for wavelength division demultiplexing. A linear substrate surface hologram array is further employed to convert the substrate guided modes into a linear array of surface-normal beams. A look-down photodetector array can be stacked on the surface of the device substrate with effective optical coupling and aligning.

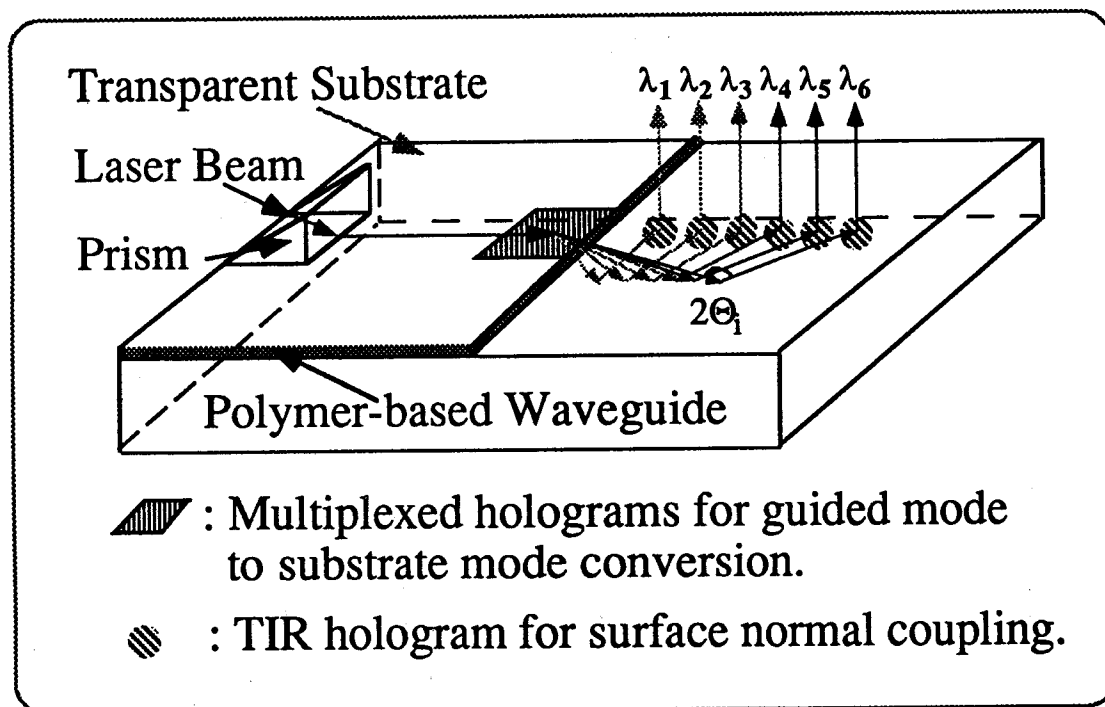


Figure 1: Schematic diagram of the in-plane to surface-normal optical WDDM.

There are two types of holograms involved in this optical surface-normal WDDM. The first type, planar waveguide multiplexed holograms (see Fig. 1), diffract the planar guided wave into many substrate modes, corresponding to different wavelengths, respectively. The second type of hologram, the TIR hologram, is a transmission hologram which can convert a substrate guided mode into a surface-normal output beam. Using dichromate gelatin (DCG), a photolime gel polymer doped with ammonium dichromate (~4%  $(\text{NH}_4)_2\text{Cr}_2\text{O}_7$ ), up to 60 planar waveguide holograms can be recorded in the same emulsion area due to the large index modulation<sup>[5]</sup> (up to 0.2). Nearly 100% optical coupling efficiency can be achieved with a hologram interaction length of 1 mm<sup>[5]</sup>. For the second type TIR hologram, optical coupling efficiency as high as 82% has been reported<sup>[7]</sup>.

A multiplexed waveguide hologram (shown in Fig. 1) is designed to diffract a planar guided wave, carrying wavelength  $\lambda_i$ , into the substrate with a bouncing angle  $\Theta_i$ , satisfying

$$\Theta_i = \tan^{-1}[i] \quad i = 1, 2, 3, 4, 5, \text{ and } 6. \quad (1)$$

As the result, a uniform separation between the two nearest surface-normal beams can be obtained as

$$S = 2d[\tan(\Theta_i) - \tan(\Theta_{i-1})] = 2d, \quad (2)$$

where  $d$  is the thickness of glass substrate. Both the thickness,  $d$ , and bouncing angle,  $\Theta_i$ , can be chosen to have the spatial separation ( $S$ ) matching the detector-detector separation. Note that the bouncing angle,  $\Theta_i$ , is designed to be larger than the critical angle ( $41.8^\circ$ ) of TIR within the optical glass substrate ( $n = 1.5$ ).

The thickness of the single-mode waveguide can be found by employing the Helmholtz beam propagation method<sup>[8]</sup> and/or the effective index method<sup>[9]</sup>, when the indices of polymer, substrate and operating wavelength are known. In many situations, multimode waveguides may have to be chosen due to their large waveguide cross section to facilitate optical coupling.

Design of the waveguide holograms is accomplished by constructing a grating vector such that a specific phase matching condition can be met. For the waveguide holograms employed herein, most of the theory can be borrowed from the well-developed theories for holographic gratings<sup>[10,11]</sup>. The multiplexed holograms employed here are formed by sequentially recording single gratings that have been designed operating at a specific Bragg diffraction angle and a specific wavelength.

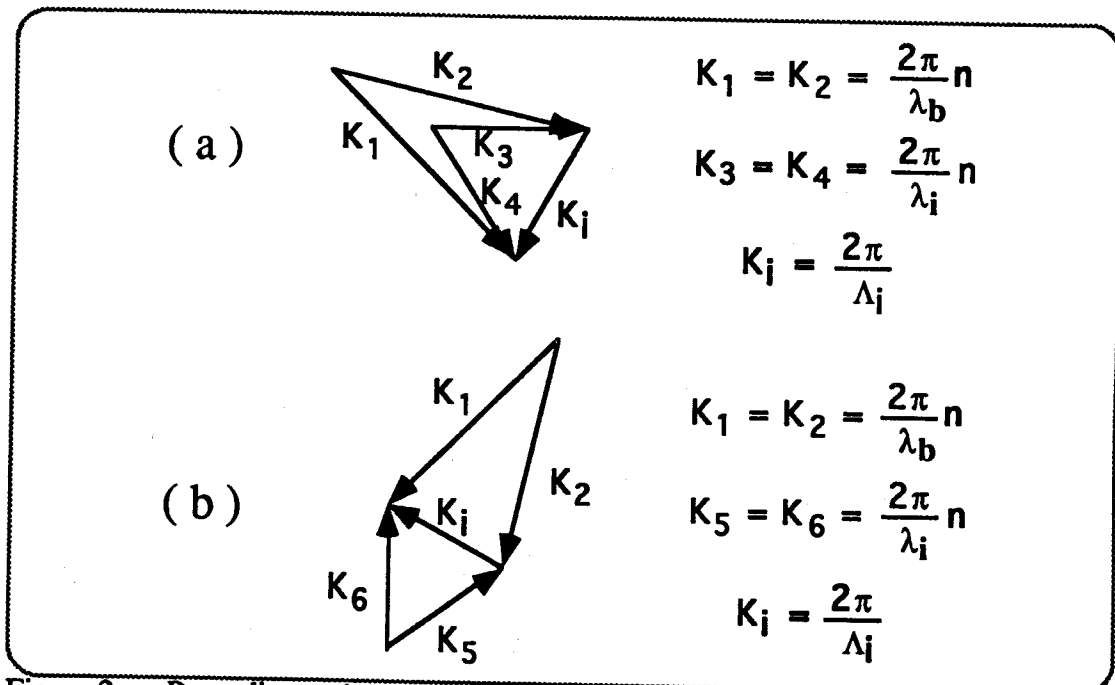


Figure 2: Recording and reconstruction phase-matching diagrams for (a) multiplexed holograms, and (b) TIR holograms. Here,  $\lambda_b$  = recording wavelength,  $\Lambda_i$  = grating spacing.  $n$  = holographic polymer index.

To construct the two types of holograms employed, the recording and reconstruction conditions shown in Fig. 2(a) and 2(b) are required. Because of the strong blue absorption band of the holographic material (DCG), we choose  $\lambda = 488$  nm as the recording wavelength provided by an Ar<sup>+</sup> laser (INNOVA 200). The reconstruction wavelengths can be designed in a wide range from 500 nm to 1500 nm, which can be different from the recording wavelength. The discrepancy for recording and reconstruction phase-matching condition for the waveguide multiplexed holograms is indicated in Fig. 2(a), while that for TIR substrate hologram is illustrated in Fig. 2(b). In Fig. 2,  $K_1$  and  $K_2$  are the propagation vectors of the two recording beams.  $K_3$  and  $K_4$  are the propagation vectors of the guided transmission wave and diffracted wave, respectively.  $K_i$  is the holographic grating vector associated with the wavelength  $\lambda_i$ .  $K_5$  is the propagation vector of the substrate transmission wave through TIR, and  $K_6$  is propagation vector of the surface-normal diffracted wave. The refractive index ( $n = 1.5$ ) of the holographic polymer is selected to match the index of glass substrate. Such index match is important to reduce the undesired interface reflection.

The techniques to construct the multiplexed waveguide holograms and TIR hologram array can be found in our previous publications[5,11,12]. The multiplexed waveguide holograms demultiplex each transmission wave of wavelength  $\lambda_i$  into a substrate guided mode with a diffraction angle  $\xi_i$ . The TIR substrate waveguide hologram converts a substrate mode with bouncing angle,  $\Theta_i = 90^\circ - \xi_i$ , into a surface-normal output beam. Note that each TIR hologram is not multiplexed in space (shown in Fig. 1), diffracting only one substrate mode at a given wavelength into a surface-normal beam.

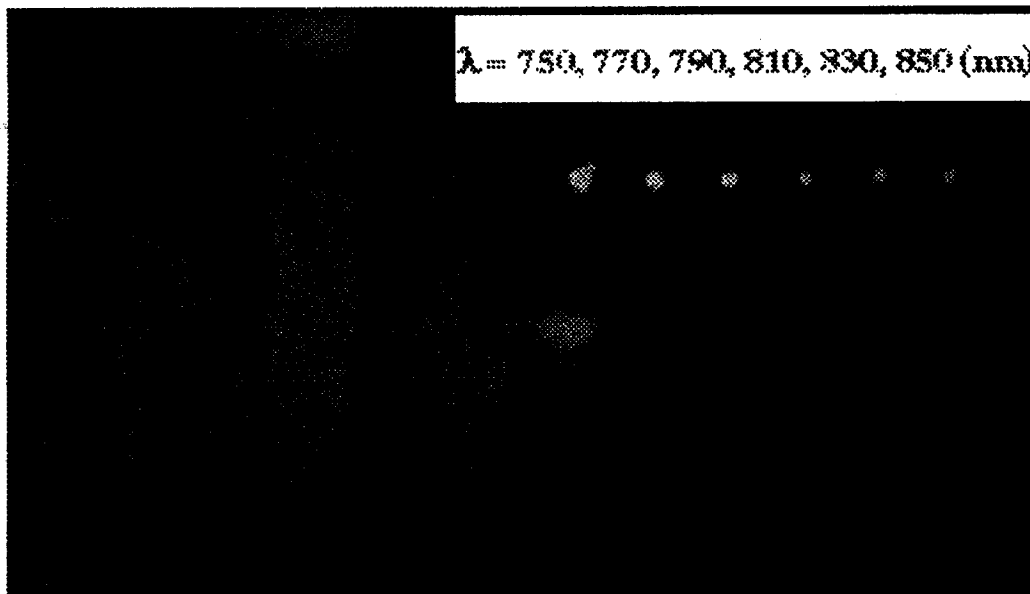


Figure 3: Photograph of the six-channel WDDM with the optical in-plane to surface-normal conversion. The near field profiles of the six surface-normal demultiplexed beams are also shown. The separation between two nearest beams is 2 mm.

Six waveguide holograms are superimposed at the end of a polymer-based planar waveguide as shown in Fig. 1. The planar guided wave having six different wavelengths

are converted into an array of six substrate guided beams with six different bouncing angles. The waveguide fabricated had thickness of  $\sim 7 \mu\text{m}$  with four possible modes of operation. The bouncing angles are fabricated according to Eq. (1) for wavelengths  $\lambda_i = 750, 770, 790, 810, 830, 850 \text{ nm}$ , respectively. An optical glass, BK-7 with the index match to the polymer ( $n = 1.5$ ), was employed as the substrate with thickness of 1 mm. Reconstruction of the surface-normal optical demultiplexer is shown in Fig. 3, where the near field pattern of the six surface-normal beams, projected surface-normally from the substrate surface, is also shown on the top of Fig. 3. The six input laser beams with  $\lambda_i = 750, 770, 790, 810, 830, 850 \text{ nm}$  are provided by a Titanium: Sapphire tunable laser (Coherent 870). Prism coupling technique is employed to couple the input laser beam into the planar waveguide. And the phase matching angle of the input is set for the  $\text{TE}_0$  mode of the planar waveguide.

The measured throughput efficiency ( $10\log_{10}[P_{\text{out}}/P_{\text{in}}]$ ) for the six surface-normal beams is shown in Fig. 4. Variations among of the six channels is within 1.5 dB. The measured coupling efficiency of the six TIR holograms are all above 50%. The coupling efficiency could be improved by using thicker holographic emulsion. The diffraction efficiencies of the multiplexed waveguide holograms were in the range of 18% to 25%. Precise control of the hologram recording process are important for uniform diffraction efficiencies.

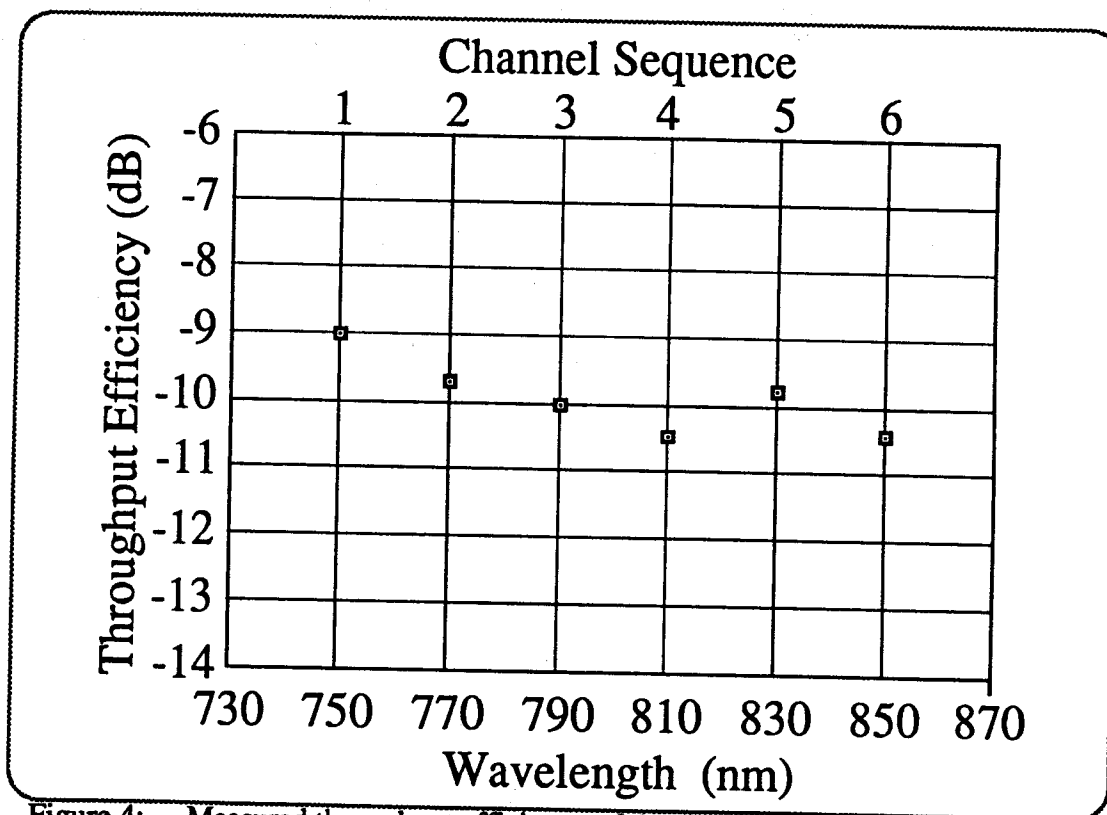


Figure 4: Measured throughput efficiency of the six surface-normal demultiplexed beams with 3.5 mW input at each given wavelength.

In many situations, 1-to-many, many-to-1, and many-to-many single wavelength fanout interconnects are needed for many existing interconnect hierarchies such as module to module, backplane and machine-to-machine interconnects. Holographic optical elements

turn out to be one of the most promising tools to provide high fan-out capability. Tree and star couplers can only provide fan-out with small fan-out angles while holographic gratings can give us much larger fan-out angles (up to  $2\pi$ ) in three-dimension. Therefore, the number of fan-outs and the angular dynamic range are much higher when using holographic gratings.

Figure 5 is the measured diffraction efficiency of an one-to-twelve surface normal fan-out interconnect working at single wavelength of  $0.6328 \mu\text{m}$ <sup>[12]</sup>. The undiffracted guided wave and the diffracted substrate waves were propagating collinearly. In this device, the linear substrate (surface-normal) hologram array are made out of identical holograms. Therefore, the device is easier to be fabricated than that shown in Fig. 1. The first ten fan-out channels have a relatively uniform intensity and the performance of the 11th and the 12th fan-out channels are relatively poor, compared with the first ten channels. Variation of the first ten channels is within 1 dB while the last two channels have a deviation of 7.2 dB and 4.5 dB, respectively. As far as the diffraction efficiency of the TIR hologram is concerned, the measured values of 12 holograms are all above 70%.

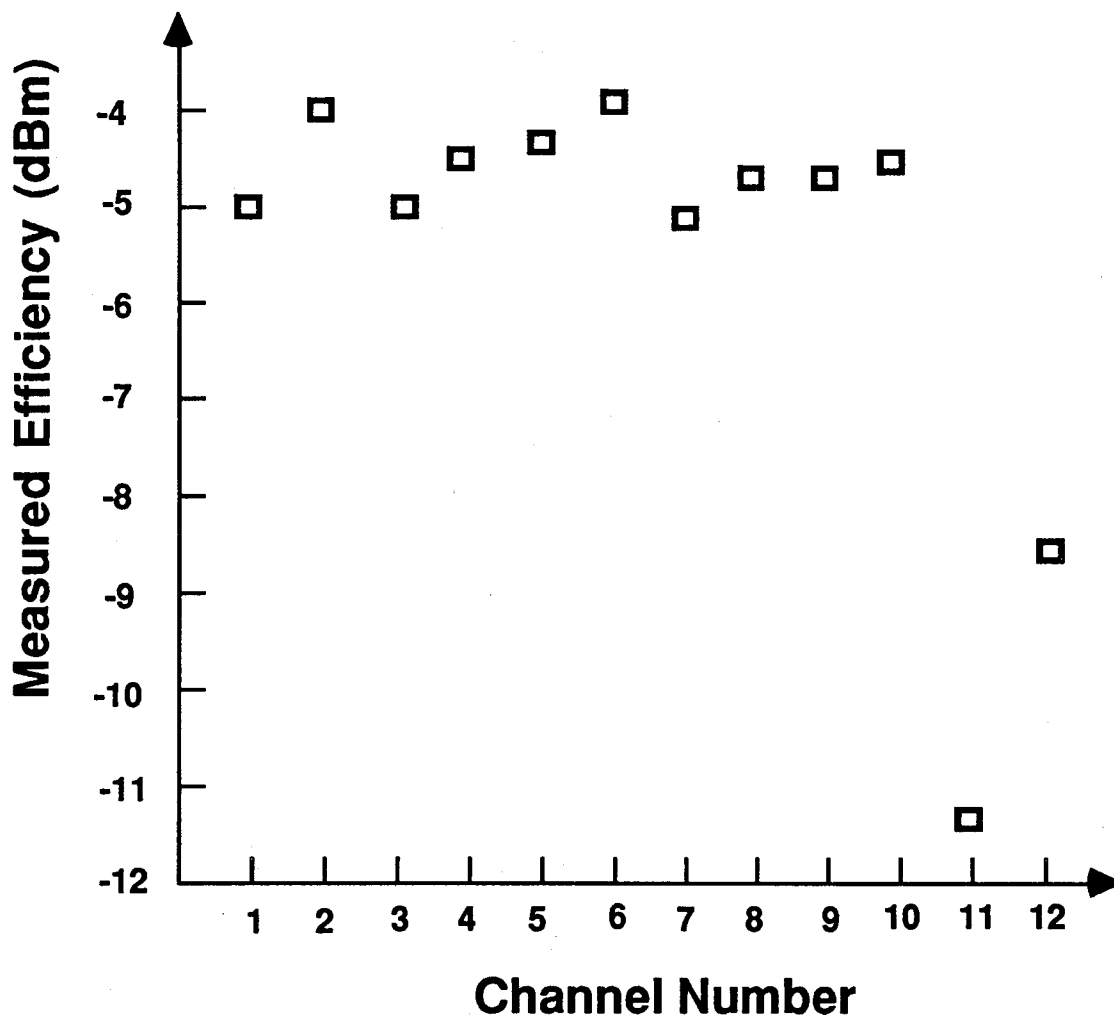


Figure 5: Measured throughput efficiency of the twelve surface-normal beams at wavelength of  $0.6328 \mu\text{m}$  (Ref. 12).

In summary, we have investigated the first six-channel WDDM with optical in-plane to surface-normal conversion for effective coupling and reliable packaging. Two types of waveguide holograms were employed on the same surface of substrate where the planar waveguide is fabricated. The non-uniformity of the throughput efficiency among the demultiplexed surface-normal beams is determined to be within 1.5 dB. This result represents an effort to eliminate the two dimensional nature of conventional planar lightwave circuits. Such a surface-normal WDDM provides an effective optical face-to-face coupling and packaging for a photodetector array. Based on this novel optical in-plane to surface-normal conversion, advanced technologies including vertical cavity surface emitting laser<sup>[13]</sup>, flip-chip bonding, thin film lift-off devices<sup>[14]</sup> and the optical fiber v-groove bounding technique<sup>[15,16]</sup> can be directly employed to fabricate cost-effective, compact optoelectronic integrated circuits for advanced optical fiber networks employing WDM. Fig. 6 shows an example of a compact optoelectronic interconnect for effective coupling and packaging between an optical fiber and a VCSEL array or a photodetector array.

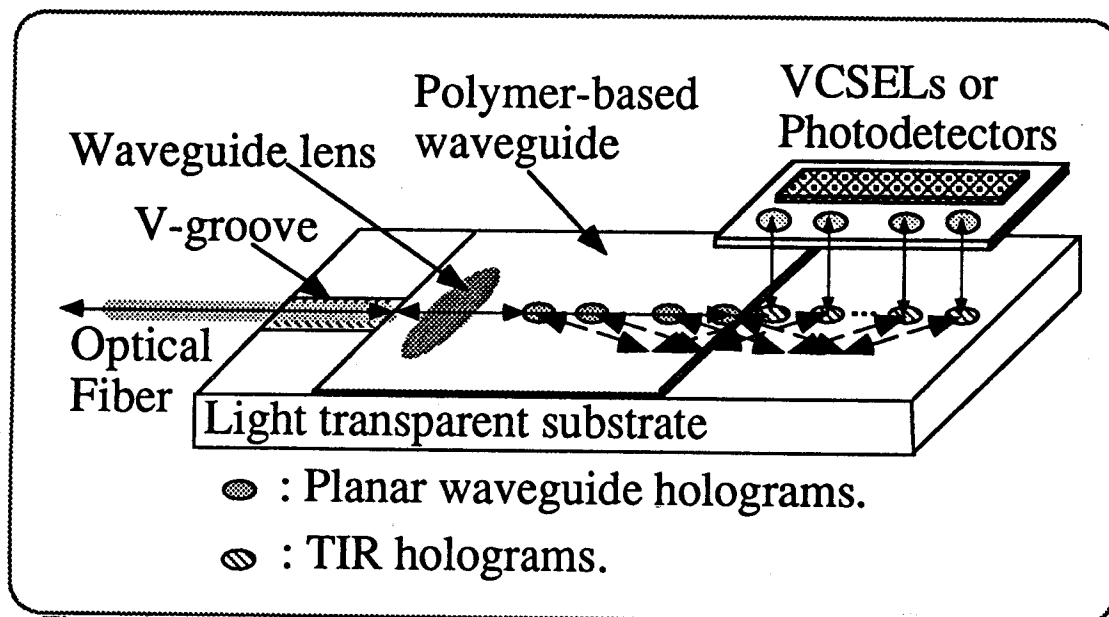


Figure 6: Compact optical interconnect for effective coupling and packaging between an optical fiber and photodetector array (or a VCSEL array).

This research is sponsored by AFOSR, BMDO, ARPA, and Cray Research, Inc..

## References

1. B. H. Verbeek, C. H. Henry, N. A. Olsson, K. J. Orlowsky, R. F. Kazarinow, and B. H. Johnson, "Integrated four-channel Mach-Zehnder multi/demultiplexer fabricated with phosphorous doped SiO<sub>2</sub> waveguides on Si," *J. Lightwave Tech.* vol. 6, pp. 1011-1015, 1988.
2. Norio Takato, Toshimi Kominato, Akio Sugita, Kaname Jinguji, Hiromu Toba and Masao Kawachi, "Silica-Based integrated optic Mach-Zehnder multi/demultiplexer family with channel spacing of 0.01-250 nm," *IEEE J. on Selected Areas in Communications*, vol. 8, pp. 1120-1127, 1990.
3. M. Zirngibl, M. D. Chien, U. Koren, C. H. Joyner, B. I. Miller, M. G. Young, H. M. Presby, J. Meester, L. W. Stulz, "An integrated seven channel WDM receiver," *OSA/IEEE Tech. Dig. Series*, vol. 3, pp. 207-209, 1994.
4. M. Zirngibl, C. H. Joyner, L. W. Stulz, Th. Gaiffe, C. Dragone, "Waveguide grating demultiplexer on InP," *Electron Lett.*, vol. 29, pp. 207-209, 1993.
5. Ray T. Chen, "Near Infrared 12-Channel Wavelength Division Demultiplexer on a semi-insulating GaAs Substrate," 1993 OSA Topical Meeting on Integrated Photonics Research, IME-3, pp. 18-21, (1993).
6. J.-M. Verdiell, T. L. Koch, B. I. Miller, U. Koren, M. G. Young, F. Storz, K. F. Brown-Goebeler, "An integrated WDM receiver with net gain on InP," *OSA/IEEE Tech. Dig. Series*, vol. 3, pp. 210-212, 1994.
7. Michael R. Wang and Tomasz Jansson, "Substrate wavelength-demultiplexing optical interconnects based on superimposed holographic gratings and three-dimensional Bragg diffraction," *Opt. Lett.*, vol. 18, pp. 2068-2070, 1994.
8. Matthew R. Fetterman and Stephen R. Forrest, "Modeling of a waveguide device using the Helmholtz beam propagation method," *OSA/IEEE Tech. Dig. Series*, vol. 3, pp. 51-56, 1994.
9. B. Hocker and W. K. Burns, "Mode dispersion in diffused channel waveguides by the effective index method," *Appl. Opt.*, vol. 16, pp. 113-117, 1977.
10. H. Kogelnik, "Coupled wave theory for thick hologram gratings," *Bell Sys. Tech. J.*, vol. 48, pp. 2909-2947, 1969.
11. M. R. Wang, G. J. Sonek, R. T. Chen, and T. Jansson, "Large fan-out optical interconnects using thick holographic gratings and substrate wave propagation," *Appl. Opt.* vol. 31, pp. 236-251, 1992.
12. R. T. Chen, Suning Tang, Maggie M. Li, David Gerald and Srikanth Natarajan, "1-to-12 surface normal three-dimensional optical interconnects," *Appl. Phys. Lett.*, vol. 63, no. 14, Oct., 4, pp. 1883-1885, 1993.
13. D. Vakhshoori, J. D. Wynn, and G. J. Zydzik, R. E. Leibenguth, "8x18 top emitting independently addressable surface emitting laser array with uniform



threshold current and low threshold voltage," *Appl. Phys. Lett.*, vol. 62, pp. 1718-1720, 1993.

14. Stuart K. Tewksbury and Lawrence A. Hornak, "Multichip Modules: A platform for optical interconnections within microelectronic systems," *Optoelectronics: Device and Technol.*, vol. 9, pp. 55-80, 1994.
15. M. F. Grant, S. Day, R., Belerby and T. Bricheno, "Low-loss coupling of ribbon fibers to silica-on-silicon integrated optics using preferentially etched V-grooves," *OSA/IEEE Tech. Dig. Integrated Photonics Research 92*, 1992, paper TuD6-1.
16. B. L. Booth, J. E. Marchegiano, C. T. Chang, R. J. Furmanak, D. M. Graham, "Polymer waveguides for optical interconnect applications," *OFC Technical Dig. 94*, vol. 4, pp. 74-75, 1994.